American Mineralogist, Volume 75, pages 731–738, 1990

Polyhedral rationalization of variation among the single-crystal elastic moduli for the upper-mantle silicates garnet, olivine, and orthopyroxene

SHARON L. WEBB,* IAN JACKSON
Research School of Earth Sciences, P.O. Box 4, ANU, Canberra, ACT, Australia

ABSTRACT

Examination of the variation in elastic properties of minerals of a range of structures and compositions reveals that crystal structure plays the primary role in determining the relative magnitude of elastic properties, with compositional changes within a crystal structure being responsible for second-order variations in the observed elastic properties. Comparison of the elastic compliances of garnet, olivine, and orthopyroxene (of approximate upper-mantle compositions) and their respective pressure dependences, together with examination of the structure of these minerals, results in a qualitative understanding of the relationship between crystal structure and elasticity for these minerals. This approach follows that of previous studies except that attention is focused on elastic compliances rather than on elastic stiffnesses. Appreciation of this relationship between structure and elastic compliance may provide an explanation for the anomalous pressure dependence of the elastic moduli of orthopyroxene at pressures below 3 GPa ($K_0' = 10.78$, $K_0'' = -1.61$ GPa^{-1}) and indicates that the pressure dependence of the elastic moduli of orthopyroxene will be much lower at pressures >3 GPa. This illustrates the inherent difficulties in extrapolating elasticity data beyond the pressure and temperature regimes of the measurements.

INTRODUCTION

It has been demonstrated, particularly for olivine and orthopyroxene (Weidner and Vaughan, 1982; Vaughan and Bass, 1983; Bass et al., 1984), that the relative magnitudes of the stiffness or compliance moduli tend to be controlled primarily by gross features of the crystal structure, with cation composition playing a subsidiary role (see Tables 1 and 2). The Na-containing clinopyroxenes are an important exception—the interplay between composition and structure results in a wide variation of elastic moduli, especially in response to Al-Fe substitution in the M1 site (see Table 3).

The advent of high-pressure and high-temperature crystal-structure refinements has provided a firmer basis for the polyhedral view of crystal structures, along with detailed information concerning apparent polyhedral compressibilities and expansivities (e.g., Hazen and Finger, 1978, 1980, 1981; Levien and Prewitt, 1981). These factors, along with the inherent difficulty of ab initio and atomistic approaches to the elasticity of these complex crystal structures, have led to both qualitative and quantitative (Weidner and Vaughan, 1982; Vaughan and Bass, 1983) discussion of crystal elasticity in terms of polyhedral models. Cation- and Si-centered polyhedra of known relative rigidities and compressibilities are thus regarded as the basic building blocks for the structure and are linked (e.g., by corner, edge, and face sharing) to form structural elements (such as chains, columns, and layers) whose mechanical properties provide at least a qualitative explanation of many of the major features of crystal elasticity.

The elasticity of a crystal may be described in terms of either the compliances or the stiffnesses of the structural elements (e.g., Nye, 1957). The elastic stiffness moduli c_{ij} arise naturally in the context of wave propagation because of their close relationship to the wave-velocity eigenvalues. The c_{ij} determine the stresses required to produce a simple one-component strain ϵ_j. It is more appealing in the present discussion to emphasize the elastic compliances s_{ij}, which yield the strains arising from the application of a simple one-component stress.

The following discussion attempts to identify the important structural elements in garnet, olivine, and orthopyroxene and to assess their influence on the elasticity of these minerals. This approach follows that of Weidner and colleagues, except that attention is focused on the elastic compliances of the minerals rather than on the elastic stiffnesses. Many of the principal conclusions concerning the relative magnitudes of the compressional and shear moduli have previously been drawn by Weidner and his collaborators. However, the arguments concerning the off-diagonal moduli and the anomalous pressure dependence of the orthopyroxene compressional moduli represent a significant extension of this earlier work.

In their discussions of the elastic properties of polyhedral models for crystal structures, Vaughan and Weidner (1978), Bass (1982), Weidner and Vaughan (1982),

* Present address: Bayerisches Geoinstitut, Universität Bayreuth, Postfach 10 12 51, 8580 Bayreuth, West Germany.

0003–004X/90/0708–0731$02.00

TABLE 1. The zero-pressure elastic compliances of a number of olivines (in units of 10^{-3} GPa^{-1})

	Fo 1	Fo 2	$Fo_{92.7}$ 1	$Fo_{90.5}$ 3	$Fo_{87.8}$ 4	Fa 5	Fa 6	Mn 6	Co 6	Ni 7
s_{11}	3.4	3.5	3.4	3.5	3.6	4.8	4.9	5.0	4.2	3.7
s_{22}	5.9	5.8	6.0	6.1	6.3	9.1	8.3	8.7	7.3	5.7
s_{33}	5.0	4.9	5.0	5.1	5.0	5.9	5.7	6.9	5.9	5.3
s_{44}	15.2	14.9	15.5	15.8	15.6	31.7	30.9	22.1	21.4	14.1
s_{55}	12.3	12.3	12.8	13.0	12.4	21.4	21.4	18.0	15.7	11.5
s_{66}	12.4	12.3	12.7	12.8	13.9	17.5	17.5	17.3	15.4	12.8
s_{12}	−0.8	−0.9	−0.9	−0.9	−1.1	−2.3	−2.0	−1.8	−1.5	−1.2
s_{13}	−0.7	−0.7	−0.8	−0.7	−0.6	−0.9	−1.2	−1.5	−1.2	−1.1
s_{23}	−1.6	−1.5	−1.7	−1.8	−1.8	−2.7	−2.6	−3.0	−2.5	−2.0

Note: References are indicated by numbers in the column headings: (1) Kumazawa and Anderson (1969), (2) Graham and Barsch (1971), (3) Webb (1989), (4) Yeganeh-Haeri and Vaughan (1984), (5) Graham et al. (1982), (6) Sumino (1979), (7) Bass et al. (1984).

and Weidner et al. (1982) formulated the following set of basic rules for the relationships between the crystal compliances and the compliances of the major structural elements making up the crystal:

1. When the compliance of a structure is measured parallel to a set of structural elements, the least compliant element will determine the overall compliance in that direction.

2. When compliance is measured as normal to a set of structural elements, the compliance is determined by the most compliant element.

3. The structural compliances defined in this manner can be increased by the introduction of polyhedral linkages with rotational degrees of freedom.

These simple rules for the determination of the relative compliances of structural elements shall be employed in the following discussion of the compliances of the minerals garnet [$(Mg_{0.62}Fe_{0.36}Ca_{0.02})_3Al_2Si_3O_{12}$], olivine ($Fo_{90.5}$), and orthopyroxene ($En_{80}$), recently measured as functions of pressure to 3 GPa (Webb, 1989; Webb, unpublished data).

ZERO-PRESSURE COMPLIANCES

Compressional compliances

Uniaxial stresses σ_i (i = 1, 2, 3) and the associated strains ϵ_i determined by the compressional compliances s_{ii} are the most readily envisaged and will be discussed first. These compressional compliances for the garnet, olivine, and orthopyroxene of the present study are listed in Table 4 in order of increasing compliance, along with information concerning the principal structural element for each case. It is immediately evident that there is an impressive correlation between increasing measured compliance and increasing inferred compliance of the principal structural element. In the upper part of the table, the compressive stresses are supported by sturdy columns or well-braced chains of relatively incompressible polyhedra, whereas the lower entries have compressive stresses oriented normal to unusually compliant layers. A number of the compliances in the center of the table are comparable, and the relatively small differences among them are beyond the resolution of this qualitative analysis. On the other hand, the low values of s_{11} for olivine and garnet and the high value of s_{22} for orthopyroxene deserve special consideration.

There are three major structural elements in the olivine structure. The first of these is the column (Fig. 1) parallel to [100] of alternate SiO_4 tetrahedra and triangular clusters of edge-sharing octahedra (2M1, 1M2). Each tetrahedron shares its basal-plane edges with the three octahedra of the cluster below (or above) and its apical corner

TABLE 2. The zero-pressure compliances of a number of orthopyroxenes (in units of 10^{-3} GPa^{-1})

	En 1	$En_{84.5}$ 2	En_{80} 3	En_{80} 4	Fs 5
s_{11}	5.3	5.2	5.2	5.4	7.3
s_{22}	6.7	7.2	7.5	7.2	10.4
s_{33}	5.2	5.4	5.2	5.2	7.0
s_{44}	12.8	12.0	12.2	12.1	17.0
s_{55}	13.2	13.1	13.3	13.1	17.2
s_{66}	12.2	12.7	12.9	12.8	20.4
s_{12}	−1.86	−1.89	−2.05	−2.19	−3.78
s_{13}	−0.85	−0.98	−0.91	−1.01	−1.82
s_{23}	−1.18	−1.21	−1.09	−1.01	−1.70

Note: References are indicated by numbers in the column headings: (1) Weidner et al. (1978), (2) Kumazawa (1969), (3) Frisillo and Barsch (1972), (4) Webb (unpublished data), (5) Bass and Weidner (1984).

TABLE 3. The zero-pressure compliances of a number of clinopyroxenes (in units of 10^{-3} GPa^{-1})

	Jadeite 1	Diopside 2	Hedenbergite 3
s_{11}	4.31	5.75	5.41
s_{22}	4.82	7.14	7.28
s_{33}	4.17	5.58	5.23
s_{44}	11.60	13.65	18.75
s_{55}	16.14	16.95	16.67
s_{66}	10.86	15.31	17.19
s_{12}	−1.38	−2.10	−1.54
s_{13}	−0.71	−1.40	−1.16
s_{23}	−1.00	−1.09	−1.99
s_{15}	0.34	−0.33	−0.23
s_{25}	−0.52	0.49	−0.39
s_{35}	−1.52	−3.10	−1.53
s_{46}	−1.60	−1.44	3.13

Note: References are indicated by numbers in the column headings: (1) Kandelin and Weidner (1988a), (2) Levien and Prewitt (1981), (3) Kandelin and Weidner (1988b).

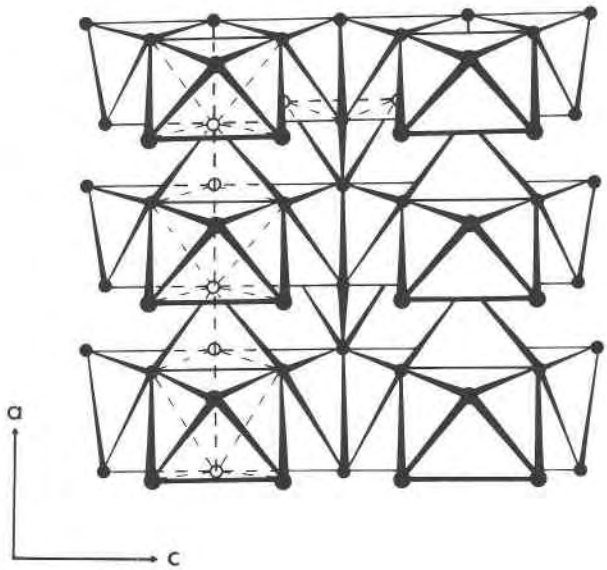

Fig. 1. A schematic view of the polyhedral linkages in the olivine structure, viewed approximately down [010] (after Hazen, 1976).

with the three octahedra of the cluster above (or below). Most of the compliance of this unit would be expected to come from the triangular cluster of octahedra rather than from the capping tetrahedron. However, the very symmetrical arrangement of short shared octahedral-octahedral and octahedral-tetrahedral edges (they define an empty tetrahedron) must confer unusually low compliance on the cluster of octahedra (Bass et al., 1984), hence the low value of s_{11}.

The second structural element of significance in the olivine structure consists of relatively straight chains of M1 octahedra that run parallel to [001]. These chains can be seen clearly in the (100) polyhedral layers of Figure 2. These chains are well braced by the linking tetrahedra in the layers above and below (Fig. 1) and also by the M2 octahedra in the same layer (Fig. 2). These braced octahedral chains parallel to [001] serve to link the previously mentioned [100] columns, thus forming (010) layers three polyhedra thick. These triple layers are joined along [010] by the sharing of a layer of M2 octahedra. The long and hence compliant unshared edges of the M2 octahedra are favorably oriented for compression or extension parallel to [010] (i.e., ϵ_2). As a consequence, these (010) layers of M2 octahedra constitute a third important structural element with considerable compliance parallel to [010]. Hazen and Finger (1980) have shown that the MO_6 octahedra in the olivine structure are compressed with increasing pressure, whereas the SiO_4 tetrahedra remain relatively incompressible. The M1 and M2 octahedra are most compressible in the [010] direction.

The load-bearing element associated with the next lowest compliance—s_{11} for garnet—is a kinked chain of alternate corner-sharing SiO_4 tetrahedra and AlO_6 octahedra running parallel to the crystallographic axes, braced by edge sharing with MO_8 dodecahedra (see Fig. 3). These chains are linked to form a three-dimensional framework that is braced against further kinking by the edge sharing of both tetrahedra and octahedra with the MO_8 dodecahedra. The edge sharing of the dodecahedra with each other and with the tetrahedra and octahedra making up the axial chains restricts the relative rotation of polyhedra within the chains. The lesser compressibility of SiO_4 tetrahedra and AlO_6 octahedra relative to MgO_6 octahedra, along with the dodecahedral bracing, explains why s_{11} for

Table 4. The compressional compliances with their first and second pressure derivatives and the principal structural elements of the garnet, olivine, and orthopyroxene structures

s_{ij}	s_{ij}	$\partial s_{ij}/\partial P$	$\partial^2 s_{ij}/\partial P^2$	Principal structural element
s_{11}*	3.5	−0.06	0.005	Columns of rigid triangular clusters of three edge-sharing octahedra (2M1, 1M2) capped by isolated SiO_4 tetrahedra sharing basal-plane edges and apical corners with the clusters of octahedra.
s_{11}**	3.8	−0.08	0.006	Chains of alternate corner-sharing SiO_4 tetrahedra and AlO_6 octahedra braced by edge-sharing distorted MO_8 dodecahedra.
s_{33}*	5.1	−0.10	0.008	Relatively straight chains of M1 octahedra well braced by edge sharing with SiO_4 tetrahedra and M2 octahedra.
s_{33}†	5.2	−0.22	0.030	Serrated chains of M1 octahedra braced by edge-sharing M2 octahedra and capped by pairs of opposed kinked and puckered A and B chains of tetrahedra (I-beams).
s_{11}†	5.4	−0.08	−0.023	Alternate layers of octahedra (M1 and M2 edge-sharing and hence relatively densely packed within the layer) and tetrahedra. Layer of tetrahedra may have finite compliance owing to the presence of the degree of freedom of movement inherent in the puckering of the chains.
s_{22}*	6.1	−0.13	0.006	Alternate layers of M2 octahedra (corner-shared and thus not densely packed within the layer) and of tetrahedra and M1 octahedra (the latter edge share with the tetrahedra).
s_{22}†	7.2	−0.31	0.056	Long bonds of the distorted M2 octahedra connected to the bridging O atoms (03) of the tetrahedra in the kinked and puckered chains capping the I-beams.

Note: Units for s_{ij}, $\partial s_{ij}/\partial P$, and $\partial^2 s_{ij}/\partial P^2$ are 10^{-3} GPa^{-1}, 10^{-3} GPa^{-2}, and 10^{-3} GPa^{-3}, respectively.
* Olivine.
** Garnet.
† Orthopyroxene.

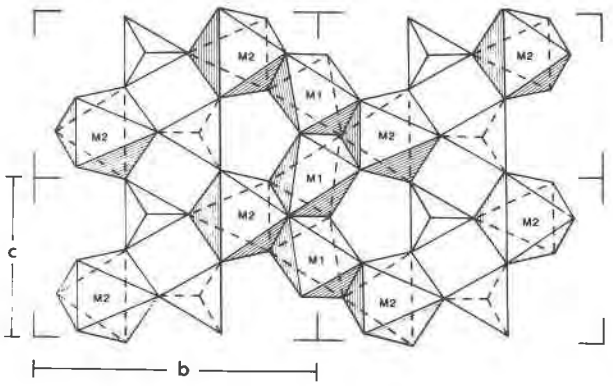

Fig. 2. A schematic view of the olivine structure viewed down [100] (after Hazen, 1976).

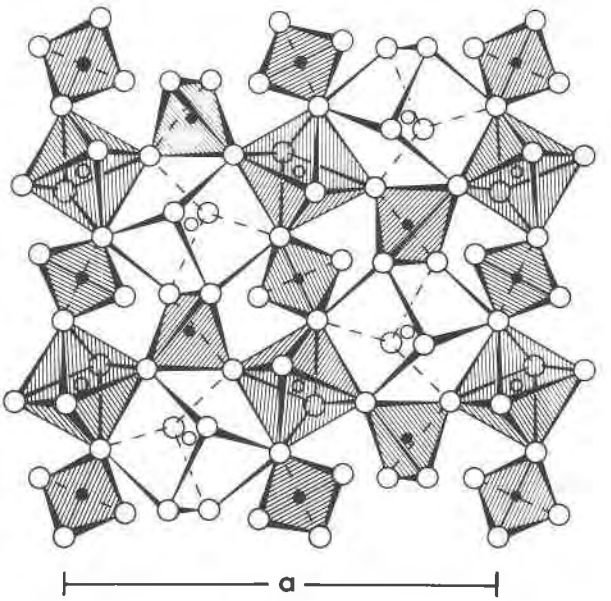

Fig. 3. The crystal structure of garnet viewed down [001] (after Novak and Gibbs, 1971).

garnet is less than s_{ii} for braced chains of MO_6 octahedra (e.g., s_{33} for olivine and orthopyroxene).

The structure of orthopyroxene consists of alternate (100) layers of SiO_4 tetrahedra and MO_6 octahedra (Cameron and Papike, 1981) (see Fig. 4). In each layer of tetrahedra, adjacent tetrahedra share corners to form distorted chains running parallel to [001]. There are two symmetrically distinct kinked chains of SiO_4 tetrahedra in the orthopyroxene structure, labeled A and B, with the B chain being the more distorted (Figs. 4 and 5). The layers of octahedra consist of small, regular M1 octahedra and larger, more distorted M2 octahedra. The M1 octahedra share edges to form serrated chains running parallel to [001]. The chains are braced by edge-sharing M2 octahedra. The M2 octahedra are situated on the outer edges of the chains of M1 octahedra. The tetrahedral basal planes are constrained to approximate parallelism with the (100) plane by their corner linkages to the M1 and M2 octahedra.

The principal element of the orthopyroxene structure is the braced, serrated chain of M1 octahedra parallel to [001], which is linked above and below to two kinked chains of tetrahedra. This element has been termed an I-beam by Cameron and Papike (1981) because of its appearance in (001) cross section (see Fig. 4). These I-beams interconnect laterally via the edge and corner sharing of the tetrahedra with the M2 octahedra and the corner sharing of the tetrahedra with the M1 octahedra (see Fig. 4). The SiO_4 tetrahedra are the least compliant polyhedra in the structure (Levien and Prewitt, 1981; Hazen and Finger, 1981), with the M2 octahedra being the most compliant. However, in this structure, relative rotation of polyhedra is also expected to contribute significantly to the overall compliance (Vaughan and Bass, 1983; Bass and Weidner, 1984).

The deformation of each chain of corner-connected SiO_4 tetrahedra is conveniently represented by two angles, θ_K and θ_P, defined in Figure 5. The bridging tetrahedral edges O3-O3 are oriented perpendicular to [100] and make an angle θ_K with [001]. Chain deformation associated with variation of θ_K will henceforth be termed *kinking*. Rigid body rotation of the tetrahedra about the bridging O3-O3 edge is described in terms of the angle θ_P between the basal plane O3-O3-O2 and (100). Such distortion of the chain will be termed *puckering*. For the A and B chains in Johnstown bronzite (Miyamoto et al., 1975), these parameters adopt the values $\theta_K = 8.3°$, $\theta_P = 3.7°$ and $\theta_K = 19.2°$, $\theta_P = 6.4°$, respectively. Calculations presented in Table 5 for a chain of regular tetrahedra illustrate the sensitivity of the chain geometry to variation of θ_K and θ_P.

The more deformed B chain kinks more with increasing pressure than the A chain (Ralph and Ghose, 1980). This kinking is accompanied by compression of the long edges of the distorted M2 octahedra (see Table 5 and Fig. 5), which therefore become more regular with increasing pressure. The B chain is linked by corner sharing only to the chains of M1 octahedra and to the M2 octahedra. The A chain, similarly linked to the chains of M1 octahedra and to the M2 octahedra by corner sharing, is also linked by edge sharing with the M2 octahedra; the tetrahedra of the B chain therefore have slightly more rotational freedom than those of the A chain.

The large compressional compliance of the orthopyroxene structure parallel to [010] is related to the nature of the lateral linkages between the I-beams, which are the principal structural elements running parallel to [001]. The I-beams are linked mainly by corner sharing between M1 and M2 octahedra associated with a given I-beam and tetrahedra belonging to the kinked and puckered chains of adjacent I-beams. The substantial compliance of the longest M2-O3 bonds and the rotational degrees of freedom associated with kinking and puckering of the

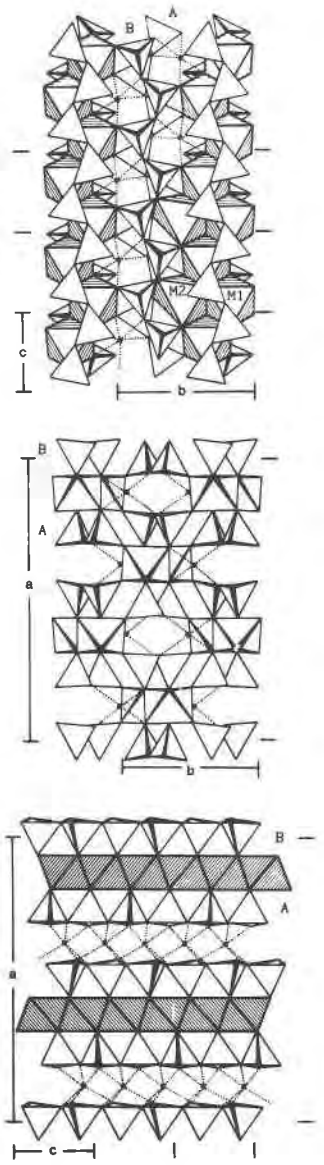

Fig. 4. The structure of orthopyroxene (after Miyamoto et al., 1975) illustrating the serrated [001] chains of M1 octahedra braced by edge-sharing M2 octahedra and capped by pairs of opposed kinked and puckered chains of tetrahedra (top), the alternate layers of edge-sharing octahedra and tetrahedra forming [100] I-beams (middle), and the long bonds of the distorted M2 octahedra connected to the bridging corners of the puckered and kinked [001] chains of tetrahedra capping the I-beams (bottom). The M2 octahedra are indicated by their M-O bonds (broken lines) except in the lower right corner of the view down [$\bar{1}$00].

tetrahedral chains account qualitatively for the high value of s_{22} (Weidner and Vaughan, 1982; Duffy and Vaughan, 1988).

The intermediate compressional compliances of Table 4 are associated with principal structural elements intermediate in character between the sturdy columns and well-braced chains of incompressible polyhedra at the top of the table and the long bonds and rotational degrees of freedom at the bottom.

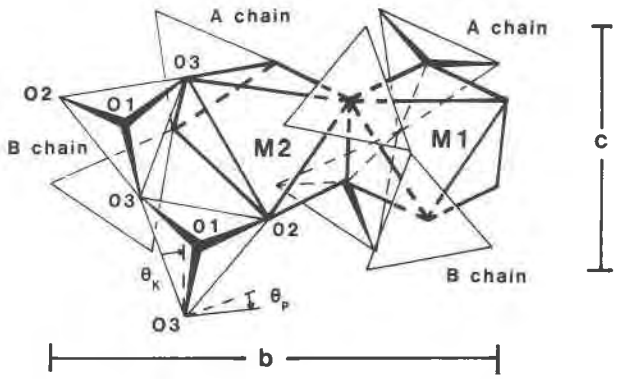

Fig. 5. The linkages of the A and B chains of tetrahedra in Johnstown bronzite to the M1 and M2 octahedra. Apical, non-bridging and bridging O atoms are denoted O1, O2, and O3 (Miyamoto et al., 1975).

Off-diagonal compliances

Table 6 lists the off-diagonal compliances of garnet, olivine, and orthopyroxene in order of increasing compliance. The relative magnitudes of these off-diagonal moduli can be discussed in terms of the magnitudes of the respective compressional compliances. For example, the application of a uniaxial compressive stress σ_1 to the olivine structure results in a small strain ϵ_1 (s_{11} is small) that is concentrated in the clusters of edge-sharing octahedra in the stiff [100] columns. The increase in energy of the octahedra due to this shortening parallel to [100] is partially compensated by extensional strains ϵ_2 and ϵ_3, and hence s_{12} and s_{13} can be inferred from the relative compressional compliances of the structural elements parallel to [010] and [001]. Accordingly, it is expected that more extensional strain will appear across the compliant layers of M2 octahedra parallel to [010] than along the [001] braced chains of octahedra, and therefore that $|s_{12}| > |s_{13}|$.

Similarly, a uniaxial compressive stress σ_2 results in thinning of the compliant layer of M2 octahedra. This deformation is accompanied by extensional strains ϵ_1 and ϵ_3 in the M2 octahedra. The fact that $s_{11} < s_{33}$ guarantees that $\epsilon_1 < \epsilon_3$ and hence that $|s_{21}| = |s_{12}| < |s_{23}|$. In the same way, the deformation experienced by the chain of M1 octahedra because of the application of a uniaxial stress σ_3 is compensated by the thickening of the layers of linking M2 octahedra, with the rigid [100] columns accommodating little strain, and thus $|s_{23}| \gg |s_{13}|$.

These three predictions of the relative magnitudes of the off-diagonal moduli form a consistent trend with

$$|s_{23}| > |s_{12}| > |s_{13}|, \quad (1)$$

which is in accord with the observed magnitudes of the off-diagonal moduli for olivine (see Tables 1 and 6).

The relative magnitudes of the compressional compli-

TABLE 5. The sensitivity of key distances to the kinking and puckering of a pyroxene-like chain of regular tetrahedra of unit side

Distance* ℓ	Angle x	Derivative** $\partial \ln \ell/\partial x$	Numerical values† (deg^{-1}) $\theta_K = 8.3°$, $\theta_P = 3.7°$	Numerical values† (deg^{-1}) $\theta_K = 19.15°$, $\theta_P = 6.4°$
a′	θ_K	0	0	0
	θ_P	$\cot(\theta_1 + \theta_P)$	1.07×10^{-2}	0.96×10^{-2}
b′	θ_K	$-\tan \theta_K$	-0.25×10^{-2}	-0.61×10^{-2}
	θ_P	$-\tan \theta_P$	-0.11×10^{-2}	-0.20×10^{-2}
c′	θ_K	$-\tan \theta_K$	-0.25×10^{-2}	-0.61×10^{-2}
	θ_P	0	0	0
O1-O1 (M1 edge)	θ_K	$-\tan \theta_K$	-0.25×10^{-2}	-0.61×10^{-2}
	θ_P	$\dfrac{3 \sin 2(\theta_2 + \theta_P)}{5\text{-}3 \cos 2(\theta_2 + \theta_P)}$	1.29×10^{-2}	1.31×10^{-2}
O2-O3 (M2 edge)	θ_K	$\dfrac{-\sin 2\theta_K + \sqrt{3} \cos \theta_P \cos 2\theta_K}{2 + \cos 2\theta_K - \sqrt{3} \cos \theta_P \sin 2\theta_K}$	-1.38×10^{-2}	-2.00×10^{-2}
	θ_P	$\dfrac{(\sqrt{3}/2)\sin 2\theta_K \sin \theta_P}{2 + \cos 2\theta_K - \sqrt{3} \cos \theta_P \sin 2\theta_K}$	0.01×10^{-2}	0.06×10^{-2}

* a′, b′ and c′ are, respectively, the maximum dimensions of the repeat unit (two tetrahedra) of the chain parallel to the [100], [010] and [001] axes of Figure 5.

** $\theta_1 = \tan^{-1} \sqrt{2}$, $\theta_2 = \tan^{-1}(1/2\sqrt{2})$.

† Values of the logarithmic derivative $\partial \ln \ell/\partial x$ for (θ_K, θ_P) combinations corresponding to those of the A (8.3, 3.7) and B (19.15, 6.4) chains of Johnstown bronzite.

ances of the orthopyroxene structure can similarly be employed in the discussion of the off-diagonal moduli. A compressive stress σ_2 will result in shortening of the long compliant bonds of the M2 octahedra and associated increased kinking of the chains of tetrahedra. However, increased kinking of a chain of incompressible tetrahedra contributes equally to ϵ_2 and ϵ_3 (see b′ and c′ in Table 5) and would therefore result in $s_{23} > 0$, which is in conflict with the observations.

In an alternative scenario, the high compliance s_{22} might be related to the other rotational degree of freedom that is associated with puckering of the chains of tetrahedra (i.e., relative rotation about edges joining bridging oxygen atoms). The sensitivities of a′, b′, and c′ to variation of θ_P (Table 5) indicate that a compressive strain ϵ_2 achieved by increased puckering is accompanied by an extensional strain ϵ_1, with $\epsilon_3 = 0$. If puckering were to play a major role in the deformation, it would therefore be expected that $|s_{12}| \gg |s_{23}|$, as observed. Similarly, a strain ϵ_1 resulting from the application of a compressive stress σ_1 may be accommodated by reduction of the puckering of the chains of tetrahedra, with significant extensional strain ϵ_2, but $\epsilon_3 \sim 0$, and thus $|s_{12}| \gg |s_{13}|$. Thus, given the initial constraint of negative s_{23} and the structural behavior implied by this observation, the off-diagonal compliances form a consistent trend, with

$$|s_{12}| > |s_{13}| \approx |s_{23}|, \qquad (2)$$

in accord with the observed moduli tabulated in Tables 2 and 6.

It is the interplay between the long M2-O3 bonds and the geometry of the kinked and puckered chains of tetrahedra that results in the anomalous compliances of the orthopyroxene structure. With increasing pressure, however, the distorted M2 octahedra are known to become more regular (Ralph and Ghose, 1980) via further kinking of the chains of tetrahedra.

Shear-mode compliances

Resistance to shear (low compliance) within a particular plane implies bracing of the structure, that is, the presence of incompressible, inextensible structural elements inclined at approximately 45° with respect to the crystallographic axes that define the plane in question. Table 7 lists the shear-mode compliances of garnet, olivine, and orthopyroxene in order of increasing compliance. It is evident that the majority of the shear compliances are comparable, only s_{44} (garnet) and s_{44} (olivine) being substantially less and greater, respectively, than average.

In olivine, the highly symmetrical arrangement of shared edges associated with the capping of triangular clusters of octahedra by tetrahedra evidently results in moderate resistance to shear in planes containing [100], i.e., moderate values of s_{55} and s_{66}. The significantly higher value of s_{44} suggests that the SiO_4 tetrahedra have some degree of freedom to rotate about [100], thereby deforming the edge-sharing octahedra in the layer above or below (Bass et al., 1984).

The modulus s_{44} for garnet is the least of the shear-mode compliances. The garnet structure (see Fig. 3) is well braced against shear by the space-filling and edge-sharing dodecahedra, which act effectively as bracing components.

THE ANOMALOUS ELASTICITY OF ORTHOPYROXENE

Pressure dependence of the compressional compliances

Comparison of the pressure dependences of the compressional compliances of garnet, olivine, and orthopy-

TABLE 6. The off-diagonal compliances of garnet, olivine, and orthopyroxene with their first and second pressure derivatives

s_{ij}	s_{ij} 10^{-3} GPa^{-1}	$\partial s_{ij}/\partial P$ 10^{-3} GPa^{-2}	$\partial^2 s_{ij}/\partial P^2$ 10^{-3} GPa^{-3}
s_{13}*	−0.74	−0.155	−0.001
s_{12}*	−0.91	−0.087	0.020
s_{13}**	−1.01	−0.175	0.095
s_{23}**	−1.01	−0.002	−0.025
s_{12}†	−1.40	0.011	0.001
s_{23}*	−1.79	0.028	0.001
s_{12}**	−2.19	0.033	0.002

* Olivine.
** Orthopyroxene.
† Garnet.

TABLE 7. The shear-mode compliances of garnet, olivine, and orthopyroxene with their first and second pressure derivatives

s_{ij}	s_{ij} 10^{-3} GPa^{-1}	$\partial s_{ij}/\partial P$ 10^{-3} GPa^{-2}	$\partial^2 s_{ij}/\partial P^2$ 10^{-3} GPa^{-3}
s_{44}*	10.60	−0.172	0.015
s_{44}**	12.07	−0.325	0.048
s_{66}**	12.81	−0.449	0.057
s_{66}†	12.80	−0.398	0.045
s_{55}†	13.00	−0.302	0.030
s_{55}**	13.07	−0.442	0.082
s_{44}†	15.75	−0.647	0.070

* Garnet.
** Orthopyroxene.
† Olivine.

roxene (see Table 4), reveals that the moduli s_{22}, and to a lesser extent s_{33}, of orthopyroxene have anomalously large pressure derivatives. In order to relate this anomalous behavior to the polyhedral model of orthopyroxene, it is necessary to look first at the pressure dependences of the elastic compliances of garnet and olivine and the changes in their structures with increasing pressure.

With increasing pressure, the compliant dodecahedra of the garnet structure become more regular and thus less compliant (Hazen and Finger, 1978). This strengthening of the bracing of the chains of tetrahedra and octahedra will reduce the already low compliance s_{11}. As these AO_8 dodecahedra (and BO_6 octahedra) compress regularly, the rate of change of the pressure derivative ($\partial^2 s_{ii}/\partial P^2$) is negligible. Similarly, for the olivine structure, increasing pressure causes the slightly deformed octahedra to become more regular and thus less compliant. The regular compression of these octahedra is mirrored in the small rate of change of the pressure derivatives of the compressional moduli of olivine.

In the orthopyroxene structure, increasing pressure causes the longest bond of the distorted M2 octahedra to shorten significantly in association with further kinking of the kinked chains of tetrahedra (Ralph and Ghose, 1980). The modulus s_{11}, however, is determined by the compliances of the alternate layers of octahedra and tetrahedra in the direction normal to the layer. Pressure-induced kinking operates in the plane of the layer and is therefore unlikely to have a significant influence on s_{11}, for which a normal pressure derivative is expected.

The analysis presented in Table 5 shows that the length of the long O2-O3 edge of the M2 octahedron is particularly sensitive to variation of the kink-angle—decreasing by ~1.4 and ~2% per degree for the A and B chains, respectively. The parameters b′ and c′ are affected equally by kinking, but different sensitivities of −0.25 and −0.61% per degree apply for the A and B chains, respectively. In order that the two chains remain in register along [001] it is therefore required that the kink angle for the less-kinked A chain increase at twice the rate of θ_K for the B chain (contrary to the observations of Ralph and Ghose, 1980) or that there be significant pressure-induced changes in the relative sizes of the A and B tetrahedra.

If both kinking and puckering are allowed in the orthopyroxene structure, the b lattice parameter is reduced by both kinking and puckering, the c lattice parameter is reduced by kinking, and the a lattice parameter is increased by puckering. The long O2-O3 edge of the M2-centered octahedron is the dimension most sensitive to kinking of the chains, whereas it is insensitive to puckering.

The initial compression of the orthopyroxene structure may be accommodated by the kinking and puckering of the chains of tetrahedra with the shortening of the long M2 bonds in response to the kinking. This combination of kinking and puckering is controlled by the resistance to deformation of the appropriate M1 octahedral edge linking the apical corners of the tetrahedra.

It is proposed that this unusually large rearrangement of the three-dimensional network of polyhedra with increasing pressure causes the structure to lose very rapidly its compliance in the [010] and [001] directions (these are the directions most affected by the kinking of the chains). Thus s_{22} and s_{33} have large pressure derivatives owing to the loss of compliance in the [010] and [001] directions accompanying the kinking of the chains and the shortening of the dominantly corner-shared lateral linkages between the I-beams. The compression of the deformed M2 octahedra will rapidly reach an equilibrium with the kinking and puckering of the chains of tetrahedra, with further kinking becoming energetically unfavorable. As this situation is approached, the pressure derivatives of the moduli s_{22} and s_{33} would be expected to return to values comparable with those observed for s_{11} in orthopyroxene and for the compressional moduli of olivine. More definitive interpretation of the anomalous orthopyroxene (and possibly for other pyroxenes) must await further high-pressure refinements of the structure.

CONCLUSIONS

A qualitative understanding of the relationship between crystal structure and elastic compliance has been

developed for the minerals garnet, olivine, and orthopyroxene, based upon the simple rules of polyhedral modeling developed by Vaughan and Weidner (1978), Bass (1982), and Weidner and Vaughan (1982). Appreciation of this relationship, together with knowledge of the changes in structure in these minerals with increasing pressure, illustrates the possible errors associated with the extrapolation of elasticity data beyond the temperature and pressure regimes of the measurements.

In the case of orthopyroxene, this simple polyhedral approach to the modeling of the crystal structure reveals a plausible pressure-sensitivity of the polyhedral linkages that determine the detailed structure of the crystal. The anomalously high first- and second-pressure derivatives of the elastic compliances of orthopyroxene (with respect to garnet and olivine) result from the extreme changes in the structure of orthopyroxene with increasing pressure. In view of this changing crystal structure, the elastic compliances observed for orthopyroxene over the 0-3 GPa pressure range cannot be extrapolated beyond this limited pressure range. The similarity between the orthopyroxene and clinopyroxene structures—chains of non-compliant SiO_4 tetrahedra and deformed MO_6 octahedra—indicate that the pressure derivative of certain elastic moduli of clinopyroxene (at low pressures) would also be anomalously high, with the pressure derivatives becoming more regular at pressures approaching that of the upper mantle. A further indication of the similarity of the pressure dependences of the elastic moduli of orthopyroxenes and clinopyroxenes is illustrated by the zero-pressure compliances of a number of clinopyroxenes (see Table 3). The relative magnitudes of the compliances of these clinopyroxenes behave in a manner similar to those of orthopyroxene.

References cited

Bass, J.D. (1982) The relationship between elasticity and crystal chemistry for some mantle silicates and aluminates. Ph.D. thesis, State University of New York, Stony Brook.

Bass, J.D., and Weidner, D.J. (1984) Elasticity of single-crystal orthoferrosilite. Journal of Geophysical Research, 89, 4359–4371.

Bass, J.D., Weidner, D.J., Hamaya, N., Ozima, M., and Akimoto, S. (1984) Elasticity of the olivine and spinel polymorphs of Ni_2SiO_4. Physics and Chemistry of Minerals, 10, 261–272.

Cameron, M., and Papike, J.J. (1981) Structural and chemical variations in pyroxenes. American Mineralogist, 66, 1–50.

Duffy, T.S., and Vaughan, M.T. (1988) Elasticity of enstatite and its relationship to crystal structure. Journal of Geophysical Research, 93, 388–392.

Frisillo, A.L., and Barsch, G.R. (1972) Measurement of single-crystal elastic constants of bronzite as a function of pressure and temperature. Journal of Geophysical Research, 77, 6360–6384.

Graham, E.K., and Barsch, G.R. (1971) Elastic constants of single-crystal forsterite as a function of temperature and pressure. Journal of Geophysical Research, 74, 5949–5960.

Graham, E.K., Sopkin, S.M., and Resley, W.E. (1982) Elastic properties of fayalite, Fe_2SiO_4, and the olivine solid solution series. EOS, 63, 1090.

Hazen, R.M. (1976) Effects of temperature and pressure on the crystal structure of forsterite. American Mineralogist, 61, 1280–1293.

Hazen, R.M., and Finger, L. (1978) Crystal structures and compressibilities of pyrope and grossular to 60 kbar. American Mineralogist, 63, 297–303.

——— (1980) Crystal structure of forsterite at 40 kbar. Carnegie Institution of Washington Year Book, 79, 364–369.

——— (1981) Crystal structure of diopside at high temperature and pressure. Carnegie Institution of Washington Year Book, 80, 373–375.

Kandelin, J., and Weidner, D.J. (1988a) The single-crystal elastic properties of jadeite. Physics of the Earth and Planetary Interiors, 50, 251–260.

——— (1988b) The elastic properties of hedenbergite, $CaFeSi_2O_6$. Journal of Geophysical Research, 93, 1063–1072.

Kumazawa, M. (1969) The elastic constants of single crystal orthopyroxene. Journal of Geophysical Research, 74, 5973–5981.

Kumazawa, M., and Anderson, O.L. (1969) Elastic moduli, pressure derivatives and temperature derivatives of single-crystal olivine and single-crystal forsterite. Journal of Geophysical Research, 74, 5961–5972.

Levien, L., and Prewitt, C.T. (1981) High-pressure structural study of diopside. American Mineralogist, 66, 315–323.

Miyamoto, M., Takeda, H., and Takano, Y. (1975) Crystallographic studies of a bronzite in the Johnstown achondrite. Fortschritte der Mineralogie, 52, 389–397.

Novak, G.A., and Gibbs, G.V. (1971) The crystal chemistry of the silicate garnets. American Mineralogist, 56, 791–825.

Nye, J.F. (1957) Physical properties of crystals, 322 p. Oxford University Press, London.

Ralph, R.L., and Ghose, S. (1980) Enstatite, $Mg_2Si_2O_6$: Compressibility and crystal structure at 21 kbar. EOS, 61, 409.

Sumino, Y. (1979) The elastic constants of Mn_2SiO_4, Fe_2SiO_4, and Co_2SiO_4 and the elastic properties of olivine group minerals at high temperature. Journal of Physics of the Earth, 27, 209–238.

Vaughan, M.T., and Bass, J.D. (1983) Single crystal elastic properties of protoenstatite: A comparison with orthoenstatite. Physics and Chemistry of Minerals, 10, 62–68.

Vaughan, M.T., and Weidner, D.J. (1978) The relationship of elasticity and crystal structure in andalusite and silimanite. Physics and Chemistry of Minerals, 3, 133–144.

Webb, S.L. (1989) The elasticity of the upper mantle orthosilicates olivine and garnet to 3 GPa. Physics and Chemistry of Minerals, 16, 684–692.

Weidner, D.J., and Vaughan, M.T. (1982) Elasticity of pyroxenes: Effects of composition versus crystal structure. Journal of Geophysical Research, 87, 9349–9353.

Weidner, D.J., Wang, H., and Ito, J. (1978) Elasticity of orthoenstatite. Physics of the Earth and Planetary Interiors, 17, 7–13.

Weidner, D.J., Bass, J.D., and Vaughan, M.T. (1982) The effect of crystal structure and composition on elastic properties of silicates. In S. Akimoto and M. Manghnani, Eds., High pressure research in geophysics, Center for Academic Publication, Japan, Tokyo.

Yeganeh-Haeri, A., and Vaughan, M.T. (1984) Single-crystal elastic constants of olivine. EOS, 65, 282.

Manuscript received August 15, 1989
Manuscript accepted April 10, 1990